Localization and delocationzation of surface disordering in surface mediated melting

Xue Fan,[1,2,3] Xiaohong Chen,[2] Deng Pan,[1] Yi Liu,[1] Ping Liu,[2] and Mo Li[3,*]

[1]*Materials Genome Institute, Shanghai University, 99 Shangda Road, Shanghai 200444, China*

[2]*School of Materials Science and Engineering, University of Shanghai for Science and Technology, Shanghai 200090, China*

[3]*School of Materials Science and Engineering, Georgia Institute of Technology, Atlanta, Georgia 30332, USA*

(Received 30 June 2021; accepted 30 September 2021; published 29 October 2021)

Melting of solids usually starts with a thin liquid layer forming on the surface at temperatures below their bulk melting point. While the liquid phase formation in the so-called premelting is understood to be governed by the interface energies among the coexisting solid, liquid, and vapor phases, the influence of the underlying crystal structures on its kinetics, and atomistic mechanisms are unknown, and consequently, ignored in the theory of melting. Here we report the first observation of a strong influence of the underlying crystal structure on melting kinetics with the resulting localization and delocalization behavior of the surface disordering and the liquid layers. With increasing temperature, the surface disordering remains in the localized state with a constant thickness in fcc crystals, whereas it becomes delocalized by growing steadily into the bulk in bcc crystals. In both cases, the surface melting is found to occur with highly correlated atomic motion in the form of extended atomic chains and loops that emit from the disordered surface and transmit to the bulk. This newly discovered mechanism in surface melting is behind the surface melting kinetics: The close packed fcc crystal can effectively impede the correlated atomic motion and limit the surface disordering to only the localized region on surface, while the more openly packed bcc crystal allows for its proliferation by tunneling from the surface into the bulk of the crystals. These findings provide valuable insights for future development of new theories of crystal melting.

DOI: 10.1103/PhysRevB.104.134204

I. INTRODUCTION

Except in a few highly controlled cases to deliberately avoid heating from the surface [1,2], melting naturally starts from the surface of solids. This happens for two reasons: one is that heat needs to be transmitted from the surface to the inside, and the other is the existing disorder of the surface. As a result, surface melting occurs at a relatively lower temperature than the melting point of the bulk by first forming a surface liquid phase [3]. The existence of this thin liquid layer has fascinated scientists for ages, ranging from the explanations of ice skating to sintering particles at low processing temperatures in metallurgy [4,5]. Advanced experimental approaches indeed reveal the formation of liquid layers during the premelting process via, for example, shadowing and blocking diffraction in proton scattering [6], x-ray diffraction [7], and differential scanning calorimetry [8], just to name a few. The formation of the liquid phase is explained by a thermodynamic relationship among the surface and interface energies, i.e., $\gamma_{lv} + \gamma_{sl} \geqslant \gamma_{sv}$, where γ_{sv} is the original solid (s)-vapor (v) interface energy before the solid surface melts into a liquid, γ_{sl} the solid-liquid (l) interface energy after the liquid phase forms on the surface, and γ_{lv} the new liquid-vapor surface energy after the surface becomes liquid. The inequality indicates that once formed, the solid-liquid interface becomes unstable and propagates to the bulk upon further heating, leading to the final melting of the bulk, while the equality signals a co-existence of all three phases at premelting temperature [9]. Computer modeling provides some detailed atomic processes of premelting and confirms that the atoms on the surface become more easily agitated at the premelting temperature and the formation of a liquid layer that further grows into the bulk, resulting in bulk melting [10].

In this work, we report findings from an atomistic modeling of premelting in two typical crystalline materials that have neither been anticipated nor observed in both experiments and theories including atomistic modeling. Different from the generic picture of surface melting with a liquid layer forming and propagating straight into the bulk, we observe two rather different kinetic behaviors of the surface disordering and liquid layers before and during premelting. For fcc metals, once the surface disorder occurs, the disordered layer(s) remains in the localized state with a nearly constant thickness even upon further temperature increase; for bcc metals, it becomes delocalized by growing steadily into the bulk with the increasing temperature. This strong dependence of the surface disordered layer on the underlying crystal structure is found to be the result of the unique atomic mechanisms of surface melting that have not been known before: Rather than random, highly correlated atomic motions are observed to form in the form of extended atomic configurations (EACs) of chains and loops in surface mediated melting. These correlated atomic configurations emit from the surface disordered layer and transmit to the bulk that cause the final bulk melting. Therefore, for the close packed fcc crystals, the densely packed atomic structure

*Corresponding author: mo.li@gatech.edu

can make the propagation of the correlated atomic motions difficult, which causes the disordered layer to be localized at the surface regions. In contrast, the more open bcc crystal allows for easy proliferation of the atomic chains and loops by tunneling into the bulk of the crystals. Hence the disordered layer becomes delocalized once formed. These findings, i.e., the correlated atomic motion originated from the surface and the strong dependence of surface mediated melting on the underlying crystal structure, shed light on our understanding of surface melting, and challenge the existing theories which so far have not taken into consideration the collective atomic motion nor the dependence of the underlying crystal structure in the formulation of crystal melting.

II. METHODS

In this work, we use Cu and Ta single crystals with (100) surfaces as examples. Other surfaces, namely the (110) and (111), are also tested and the results remain qualitatively the same. Hence we only report the results from the samples with (100) surface. There are a large number of prior works on melting of Cu (100) surface that provide references for this work [11–13]. The bcc Ta has a more open atomic packing as compared to fcc Cu. The latter is about 8.8% higher in its packing density than the former. As shown below, this difference leads to the profound difference in the localization and delocalization behaviors of the surface disordered liquids in premelting and the subsequent bulk melting.

To simulate melting and the related atomic-level properties, we use the classical molecular dynamics (MD) simulation implemented via the large-scale atomic/molecular massively parallel simulator (LAMMPS) [14]. The embedded atom method interatomic interactions are used in both Cu and Ta [15,16]. For Cu, three samples with 13 950, 108 000, and 625 000 atoms were used to test the size effect. For Ta, we also examined the size effect in our previous work [17]. We found that the systems with 54 000 atoms for Ta and 108 000 atoms for Cu are sufficient that have no obvious size effect; and hence, we report our results here mostly from these samples.

Three types of samples with (100), (110), and (111) surfaces are constructed for each metal. For each sample with a specific surface, we arrange the atoms in both the fcc and bcc crystals with two surfaces exposed on two sides of the sample, while the distance between the surfaces is sufficiently large such that along the direction z of the surface normal such that the atoms on the surfaces do not interact with each other. Along the other two directions parallel to the surfaces, x and y, the atoms still retain the periodic boundary conditions.

We use the isothermal-isobaric (*NPT*) ensemble MD to simulate melting in the samples and in particular, the Nośe-Hoover method [18,19] to control temperature. The Newton equation of motion is solved numerically with a time step of 1 fs per step. After equilibration, the samples are heated from 300 K until they melt. At each time interval of 1 ps we change the temperature by about 0.1 K. We save the atomic trajectories for analysis and calculation of structures and properties. Note that since temperature T is linearly related to time t through the heating rate, the two are used interchangeably in this work.

For better reference, we list the various melting points below obtained from this work. For fcc Cu, the premelting point for (100) surface is $T_{\text{premelting}} = 1350$ K, the bulk melting point is $T_m^{\text{surf}} = 1364$ K and $T_m^{\text{bulk}} = 1555$ K [13] with and without surfaces from the MD simulations, whereas the experimental melting point is $T_m^{\text{exp}} = 1357$ K [20]; and for bcc Ta, the premelting point for (100) surface is $T_{\text{premelting}} = 2919$ K and the bulk melting point is $T_m^{\text{surf}} = 3094$ K and $T_m^{\text{bulk}} = 3430$ K [21] with and without surfaces, whereas the experimental one is $T_m^{\text{exp}} = 3290$ K [22]. For both crystals, the bulk melting points are obtained with the heating rate at 10^{11} K/s in the MD simulation of the samples with and without free surfaces. The higher bulk melting point T_m^{bulk} without the surface is caused by superheating [23]. The slight differences in the melting point with the surface present from the experiment are caused by the interatomic interactions that are fitted with other material properties.

III. RESULTS

A. Surface disordering and premelting

Our current understanding for premelting is that it starts at a lower temperature than the bulk melting point with a thin layer of liquid forming on the surface, a few atomic layers at most. For such a small or thin region, it is difficult for experimental measurement to detect the changes in the atomic structure and surface properties. In contrast, atomistic modeling enables us to track each atom and monitor the surface disordering and melting in relation to the atomic structure change. It is known that under thermal agitation, atoms start to move away from their lattice positions. To determine precisely the nature of the surface disordering and possibly melting, and the onset of surface and bulk melting, we use the following quantities.

The first is the mean square displacement (MSD) for each atom i, $\Delta r^2(t) = |\overrightarrow{r_i}(t) - \overrightarrow{r_i}(0)|^2$, where $\overrightarrow{r_i}(t)$ is the distance between the position $\overrightarrow{r_i}(t)$ at time t, or temperature T, and the initial position $\overrightarrow{r_i}(0)$ at temperature $T = 300$ K, or initial time $t = 0$. For a system at a given temperature, the MSD is calculated by taking the average over the number of atoms, $\langle \Delta r^2 \rangle(t) = \frac{1}{N}\sum_{i=1}^{N} |\overrightarrow{r_i}(t) - \overrightarrow{r_i}(0)|^2$, where N is the number of the atoms. If we chose N for the atoms on the surface layer(s), or the interior excluding the surface, or the entire sample, the MSD represents the atomic position disorder in the different regions. From the definition, the higher the temperature, the larger the MSD, and more severe the atomic position disordering.

Since the surface is only a few atomic layers thick, the change of the MSD related to the surface is relatively small if averaged over the atoms in the entire sample. To detect the local change on the surface represented by the MSD, we also use the non-Gaussian parameter [24,25] $\alpha_2 = \frac{3\langle \Delta r^4 \rangle}{5\langle \Delta r^2 \rangle^2} - 1$. Here $\langle \Delta r^2 \rangle$ and $\langle \Delta r^4 \rangle$ can be obtained from the MSD Δr mentioned above. By definition, α_2 can capture the MSD that does not follow the Gaussian distribution of the MSDs contributed from the atoms in the interior of the sample at temperatures before bulk melting. That is, as a sample with surfaces is heated up, all atoms execute MSD from their lattice position. The surface part that has larger MSD does

not follow the Gaussian distribution of the MSD dominated by the large number of atoms from the interior. This skewness can be picked up sensitively by α_2. When the large atomic displacement occurs on the surface while the atoms inside the sample still execute small displacement, the distribution of the MSD will deviate from the Gaussian, and therefore, α_2 becomes a nonzero value. From this, we can determine the onset temperature for surface disordering. In addition, at higher temperature, the atomic displacements in the entire sample become homogeneous when the bulk starts melting, then α_2 becomes zero again.

Figures 1(a) and 1(b) shows that as Cu and Ta are heated up from 300 K, the MSD increases slowly and in almost a linear fashion. Here we normalize the MSD by the nearest neighbor distances to get the relative displacement, or Lindemann parameter, δ_L. About a few hundred degrees before the bulk melting point is approached, δ_L rises up sharply, for both Cu and Ta. The values of α_2 rise up rapidly also but at much lower temperature, about 883 K, or $0.65T_m^{\text{surf}}$, for Cu and 1641 K, or $0.54T_m^{\text{surf}}$, for Ta, where T_m^{surf} is their respective bulk melting point of the samples with (100) surfaces. The rising α_2 from zero indicates that the surface regions start to disorder.

At about 1050 K, or $0.767T_m^{\text{surf}}$, for Cu and 1911 K, or $0.63T_m^{\text{surf}}$, for Ta, α_2 reaches its peak value; and precisely at this temperature, the MSD rises sharply and deviates from the (low temperature) linear trend. The values of α_2 subsequently decline after reaching the peak values. The decrease in the value of α_2 signals that the local displacement or disorder occurred on the surface region starts at 883 K for Cu and 1641 K for Ta is now weighted down by the MSD from the atoms inside the sample. The emergence of the disordering from the interior contributes to the continuously increasing MSD, and as the MSD of the interior atoms becomes more dominant, α_2 decreases. Further increase of temperature results in the disappearance of α_2 where the MSD becomes homogeneous through the samples, which corresponds precisely to the bulk melting at $T_m^{\text{surf}} = 1364$ K for Cu and $T_m^{\text{surf}} = 3094$ K for Ta [Figs. 1(a) and 1(b)].

Surface melting is previously determined by the degree of surface atomic position disorder via the MSD, or the direct visual observation of the atom trajectories [26,27], which is also shown in Fig. 1 by the atomic configurations for Cu and Ta at some representative temperatures mentioned above. One can clearly see that at the surface disorder temperature $T_{\text{surf\_dis}}$ where α_2 becomes nonzero, the atomic structure on the surfaces are actually fairly ordered, and at the temperature corresponding to the peak in α_2, the atomic position displacements in the surface as well as inside the samples get bigger, but the structures still remain crystalline. At temperatures slightly below the bulk melting point, the disorder on the surface becomes larger and deeper inside the bulk. The more random the trajectories are, the larger the MDS, and the more disordering. According to the previous works, when the MSD reaches a critical value, namely, the Lindemann critical value [28], melting is claimed.

We have shown [17] that this criterion to determine premelting, as well as bulk melting, is not only imprecise but fundamentally incorrect, since the MSD contains both the atomic position disorder and the diffusional displacement,

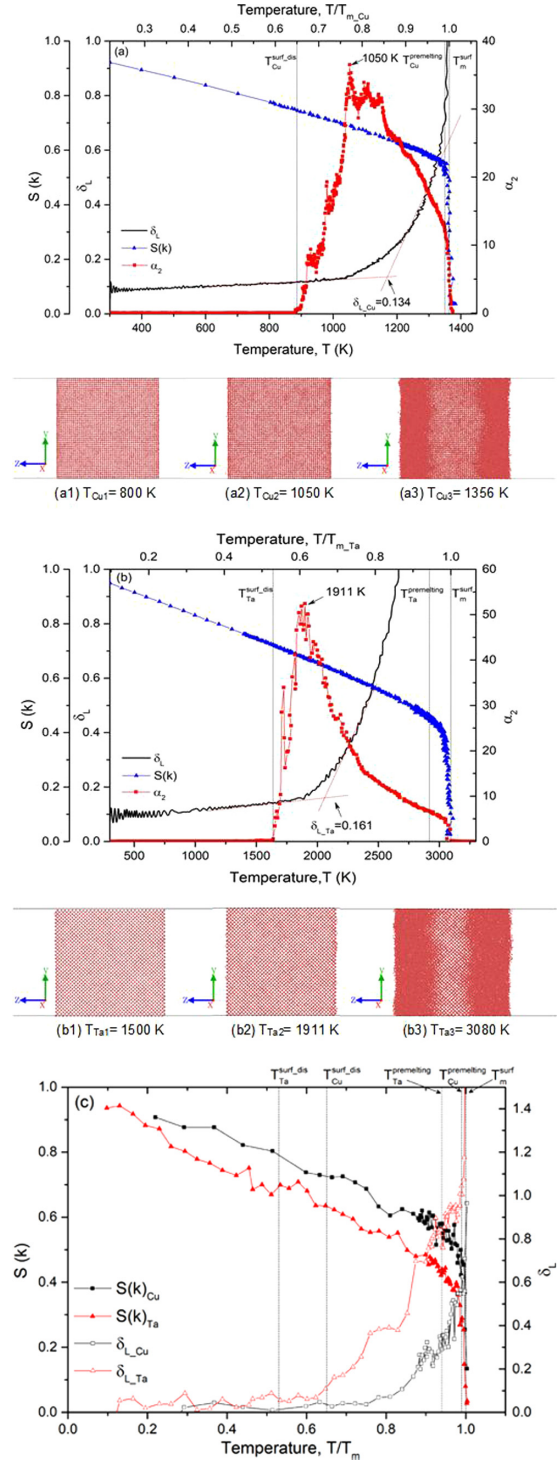

FIG. 1. The Lindemann parameter δ_L, the non-Gaussian parameter α_2, and the structure factor S(k) for Cu (a) and Ta (b) with (100) surface versus temperature (bottom x axis) and normalized temperature by the melting point (top x axis). Snapshots of the atomic configurations shown at different temperatures for fcc Cu at (a1) 800 K, (a2) 1050 K, (a3) 1356 K, and bcc Ta at (b1) 1500 K, (b2) 1911 K and (b3) 3080 K. (c) The structure factor S(k) and local δ_L for surface atoms versus normalized temperature by the bulk melting point for Cu and Ta. The surface disordering temperatures of Cu and Ta are labeled as $T_{\text{Cu}}^{\text{surf\_dis}}$ and $T_{\text{Ta}}^{\text{surf\_dis}}$, the premelting temperatures are $T_{\text{Cu}}^{\text{premelting}}$ and $T_{\text{Ta}}^{\text{premelting}}$, and the bulk melting temperature T_m^{surf}.

especially at the high temperature close to melting. The atoms engaged in diffusion jump between lattice positions does not contribute to any information of topological disorder relevant to melting [17,21]. Hence, the MSD based on Lindemann criterion cannot predict melting, which holds true here in the case of surface mediated melting for Cu and Ta. From the MSD and α_2 shown in Fig. 1, we can see that the surface becomes disordered at certain characteristic temperatures, although the surface Lindemann value δ_L is reached the value that predicts melting, for Cu, it is 0.134 at $0.86T_m^{\text{surf}}$ and Ta 0.161 at $0.64T_m^{\text{surf}}$ [Figs. 1(a) and 1(b)]. Since these δ_L are averaged in the entire sample, the Lindemann parameter may not reflect the disorder of the surfaces. Figure 1(c) shows the local MSD for the atoms only in the surface regions, about three atomic layers, during heating. Like δ_L obtained from the entire samples [Figs. 1(a) and 1(b)], the surface MSD rises up at much lower temperature, but as shown below, no premelting occurs until much higher temperatures are reached. Hence, the MSD based quantities such as δ_L tell us certain structure disordering but not melting.

To find out whether or not a liquid layer forms, that is, true surface melting, we need to use other quantities to directly probe the surface and the bulk atomic topological disordering. One is the structure factor defined as $S_i(k) = \langle \frac{1}{N^2} |\sum_{j=1}^{N} \exp(ik \bullet r_{ij})|^2 \rangle$, where $\boldsymbol{k}$ is the wavevector which is along the $\langle 111 \rangle$ directions in fcc Cu and $\langle 110 \rangle$ directions in bcc structure, r_{ij} is the nearest neighbor pair distance centered at atom i, and j that runs over all N nearest neighbors. *S(k)* defined here corresponds to the first diffraction peak with the wavevector $\boldsymbol{k}$. The value of the $S_i(k)$ is close to one in a perfect crystal and zero in liquid state. The first eight nearest neighbors of bcc Ta often become indistinguishable from those of the six second nearest neighbors when temperature is high. For this reason, we use $N = 14$ for Ta. For the atoms on the surface layer, we use the number of the actual nearest neighbors.

Figures 1(a) and 1(b) show that at 300 K, the structure factor *S(k)* for the entire samples of both Cu and Ta is about 0.9. The slight decrease from one is due to thermal agitation. As temperature increases, *S(k)* decreases smoothly; at the onset of surface disordering where α_2 becomes nonzero, *S(k)* is at about 0.8 for Cu and 0.7 for Ta, which indicates that the samples are relatively ordered despite the disordering occurring on the surfaces. The decreasing trend continues until the temperature reaches the bulk melting point where *S(k)* eventually drops to zero. Since the results are obtained by averaging over the entire sample and the surface contributes only a small portion, there is no visible drop in the value of *S(k)* before bulk melting suggesting that there is no apparent liquid phase formation at temperatures below the bulk melting point. The *S(k)* obtained in Fig. 1(c) is obtained from the atoms in the surface layers. It shows obvious decrease prior to the bulk melting. However, since the drop is too close to the bulk melting points, more direct and precise measurement is needed to find the surface premelting.

In order to obtain the structural information from the thin top layers of surfaces, we used another structure parameter, the two-dimensional radial distribution function (2DRDF) defined as $g(r, \theta) = \frac{n(r \sim r+\Delta r, \theta \sim \theta+\Delta\theta)}{A(r \sim r+\Delta r, \theta \sim \theta+\Delta\theta)\rho_0}$ for the atoms within 2 $\sim$3 top surface layers, or about 1.65 Å in thickness, where A is the area of a surface region bounded between the radial distance r and $r + \Delta r$ in the plane parallel to the surface, and polar angle θ and $\theta + \Delta\theta$; $n(r \sim r + \Delta r, \theta \sim \theta + \Delta\theta)$ is the number of atoms inside the thin slice, and ρ_0 is the mean atomic number density of the slice. The 2DRDF can give us direct information about surface disorder and liquid layer formation. Figure 2 is a series of the 2DRDFs for Cu and Ta during heating starting from 300 K to the temperatures slightly below the bulk melting point where premelting on the surface is suspected. The 2DRDFs show that the (100) surfaces in both Cu and Ta remain in a fairly ordered crystalline state up to the temperatures just slightly below the bulk melting points as evidenced by the clearly periodic patterns formed by the underlying surface crystalline structure. These crystalline patterns only begin to disappear at the premelting point $T_{\text{premelting}} = 1350$ K for Cu, about 15 K, or $T_{\text{premelting}} = 0.99T_m^{\text{surf}}$, before its bulk melting point at $T_m^{\text{surf}} = 1364$ K, and at 2919 K for Ta, which is 75 K, or $T_{\text{premelting}} = 0.96T_m^{\text{surf}}$, below its bulk melting point at $T_m^{\text{surf}} = 3094$ K. At these temperatures, the surfaces become true liquid that not only has no translational symmetry as shown in the 2DRDFs, but also no orientational symmetry [17].

B. Stability of the surface liquid phase

Our results show unambiguously that a liquid phase indeed forms in the top surface layers as suspected at the premelting temperature which is very close to the bulk melting point, particularly for Cu. The difference between the premelting temperature $T_{\text{premelting}}$ and bulk melting temperatures T_m^{surf}, $(T_m^{\text{surf}} - T_{\text{premelting}})/T_m^{\text{surf}}$, is about twice as larger for Ta as that for Cu. In other words, Ta is much easier to premelt than Cu. In the following, we shall demonstrate that this difference is in fact a manifestation of a far more profound kinetic property of the surface mediated melting dominated by the underlying crystal structures: Once the liquid layer forms, the surface becomes unstable as the samples are heated continuously. As a result, the liquid layer grows into the bulk, causing bulk melting. In the following, we focus on how the surface liquid phase, once formed, propagates into the interior of the crystals, or the kinetics of the surface mediated melting.

To monitor the motion of the surface liquid layer, we measure the atomic position disordering from the surface down to the inside of the crystals during heating. To do so, we use the atomic number density profile (ANDP). The profiles are obtained by cutting the samples into thin slices of about 1 Å in thickness at the position z parallel to the surface and counting the number of atoms in each slice. When a sample is in the ordered crystalline state, the number density exhibits periodic oscillations which reflect the underlying atomic planes; otherwise, if disordering occurs, its magnitude decreases and width broadens; and in the completely disordered liquid state, the periodic oscillation disappears. By properly identifing the position of the liquid-solid interface and its movement during heating, we can monitor the stability and movement of the surface liquid phase.

Figures 3(a) and 3(b) show the ANDPs of Cu and Ta along the direction perpendicular to the (100) surface at various

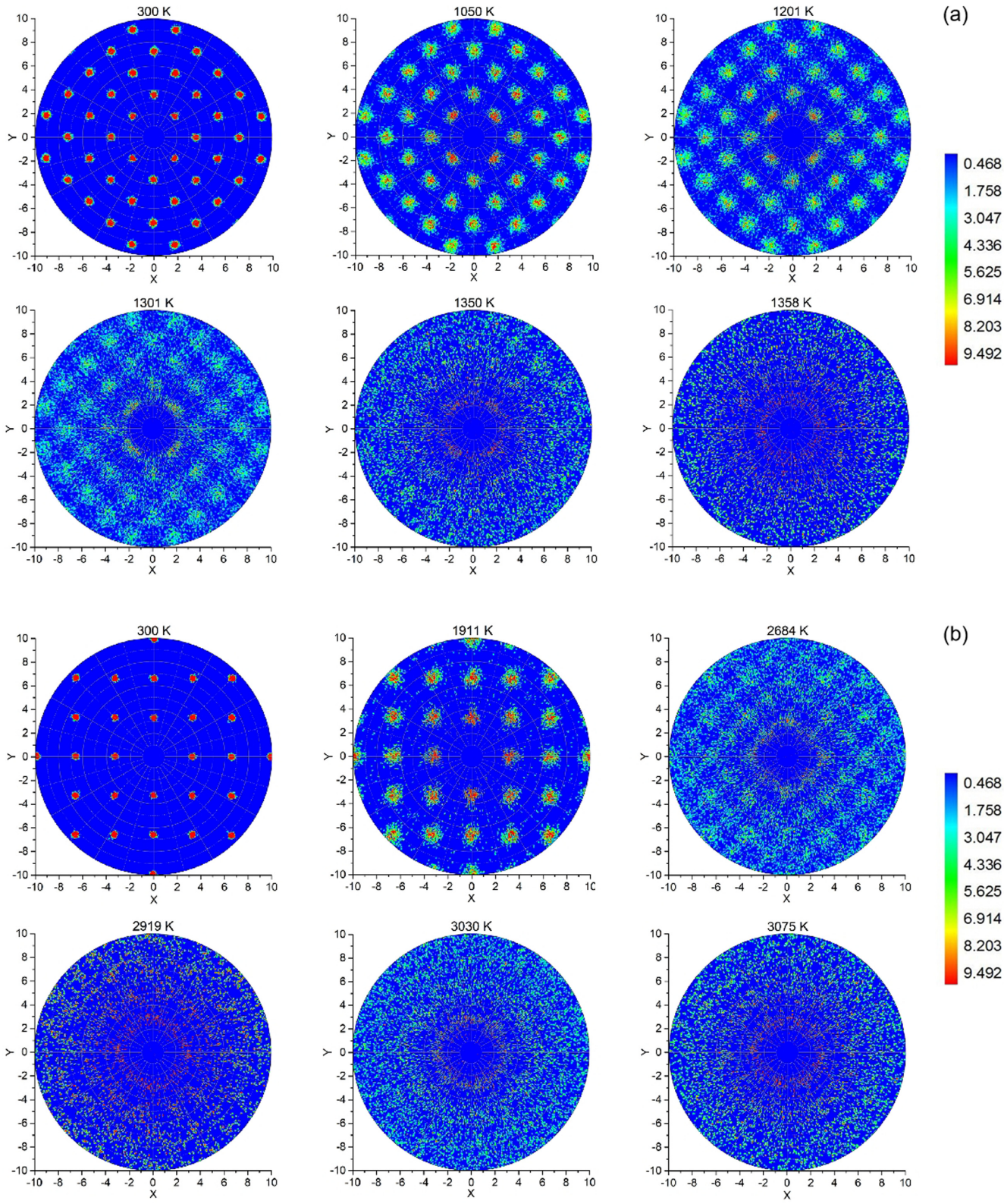

FIG. 2. The 2DRDFs for Cu (a) and Ta (b) at various temperatures.

temperatures approaching their bulk melting points. When the sample is in the ordered crystalline state, the ANDP exhibits periodic oscillations with the top surface layers having smaller magnitudes. As temperature goes up, disordering occurs and consequently, the magnitude of the density peaks decreases and width broadens; the decrease and broadening is larger for the top surface layer and the layers close to the surface than those in the interior. In the liquid state, the periodic oscillation disappears and the density approaches the mean value of the liquid phase.

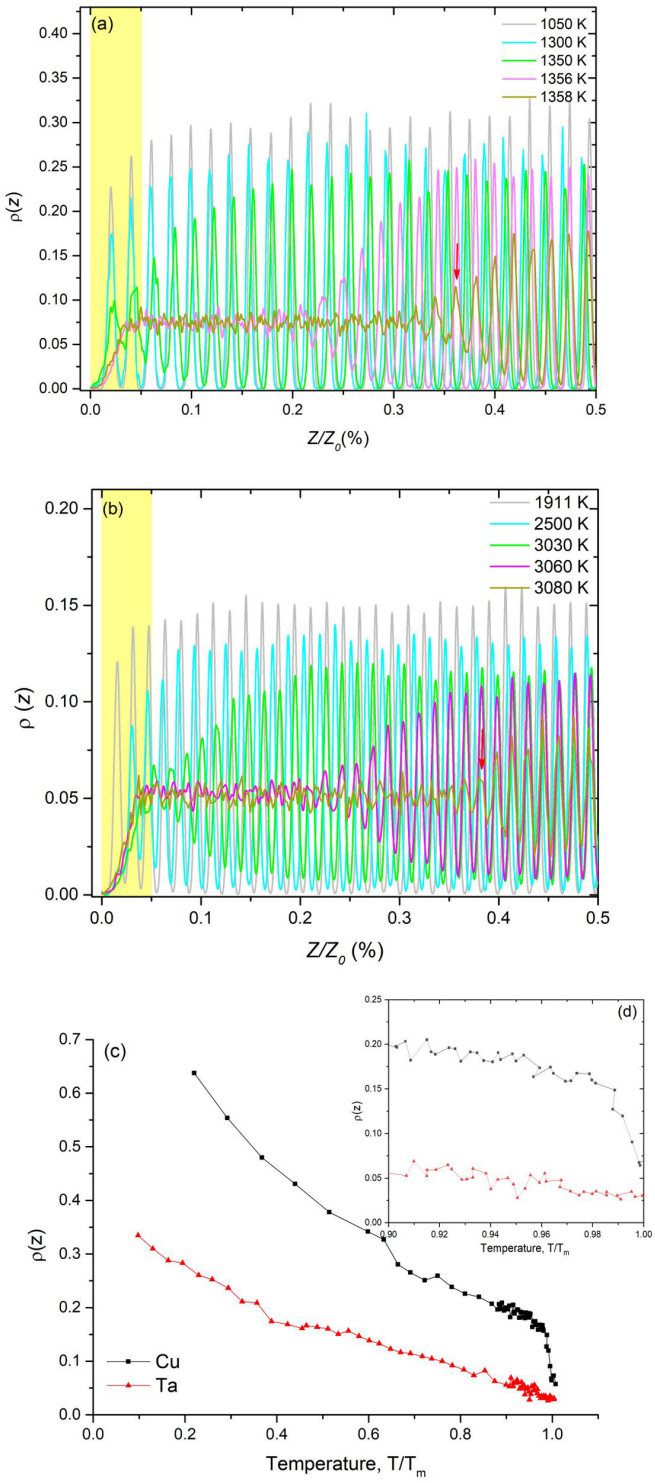

FIG. 3. The atomic number density profiles for Cu (a) and Ta (b) at different temperatures. As an illustration, we use the red arrow to mark the location of the interface between the liquid surface layer and the underlying crystal at 1358 K for Cu and at 3080 K for Ta. The bulk melting point is 1364 K for Cu and 3094 K for Ta in our MD simulations respectively. (c) The relation between the density of top 3 layers, shown in the light yellow regions in (a) and (b), versus temperature of Cu and Ta. (d) The zoom-ins of (c) close to the melting point.

Consistent with the observation in the 2DRDFs, the ANDPs of the surface layers at the temperatures below the bulk melting points indeed become flattened: for Cu it occurs around 1350∼1356 K and Ta at 2919∼3030 K [see Figs. 3(a) and 3(b)]. Figure 3(c) summarizes the change of the peak height for the top surface layers in the ANDPs at different temperatures. While it is obvious that for both Cu and Ta, the peak heights decrease with increasing temperature, Cu shows an abrupt drop at premelting whereas Ta exhibits a gradual change. To see more clearly the manner in which the drop occurs, we plot the peak heights closer to the bulk melting points in Fig. 3(d). The difference in the change of the crystalline order in premelting between Cu and Ta suggests that their surface liquid phases have different kinetic behaviors upon premelting and subsequently in causing the surface mediated bulk to melt for the two crystals with different atomic structures: For Cu, the surface layer remains relatively stable upon being heated to premelting and further to bulk melting point, whereas for Ta, the surface disorders progressively and a liquid phase forms, and at the same time pervades the bulk. In the following, we examine the movement of the liquid phase in the two systems.

C. Movement of the surface liquid phase: localization vs delocalization

From the ANDPs we can locate the liquid-solid interface at the location corresponding to the midpoint on the ANDPs that changes from the liquid to the solid phase, which is marked by a red arrow in Figs. 3(a) and 3(b). By following the movement of the interfaces at various temperature or time as we continuously heat the samples, we can measure the velocity of the interfaces. Figure 4(a) is the plot of the interface location d from the original position of the top surface layer and Fig. 4(b) is the velocity v obtained from fitting the interface positions versus time.

At low temperature, Δd is simply the mean surface positions. As the surfaces become disordered when the samples are heated up, the surfaces fluctuate and their positions expand. This is corroborated by that at the temperatures marked by the rising of the nonzero α_2 values, $\sim 0.54 T_m^{\mathrm{surf}}$ for Ta and $\sim 0.65 T_m^{\mathrm{surf}}$ for Cu as shown in Fig. 1, Δd shows a step in Fig. 4(a). As temperature increases further, Δd for Cu increases slowly, which is consistent with the observation as shown in the 2DRDFs (Fig. 2) that the surfaces experience thermal agitated disordering while still hold the crystalline order. Correspondingly, the surface shows no movement with nearly zero velocity v, or the surface disordering is localized [Fig. 4(b)]; the small, nonzero value comes from the surface expansion during heating. For Ta, the disordering region Δd becomes larger and increases steadily. At higher temperatures corresponding exactly to the premelting, both Δd and v start to rise up. In particular, for Ta the liquid phase formed on the surface layers begins to move toward the interior with an almost divergent velocity at $\sim 0.96 T_m^{\mathrm{surf}}$. In contrast, the surface phase in Cu remains stationary up to $\sim 0.99 T_m^{\mathrm{surf}}$, right before the bulk melting occurs. In other words, the surface disordering of Cu exhibits a tremendous stability, or

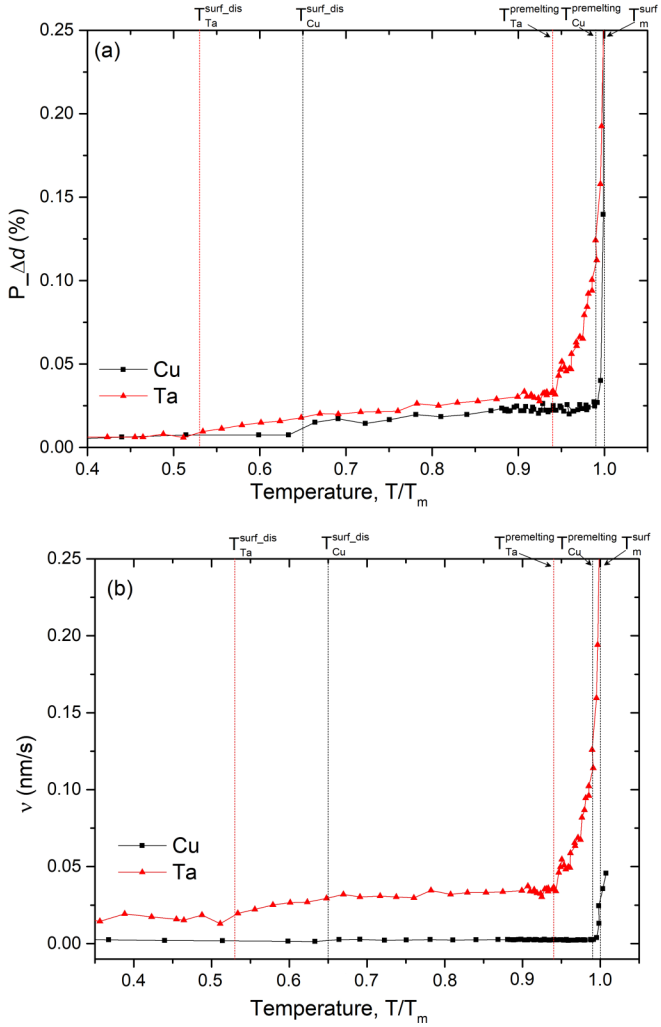

FIG. 4. (a) The thickness Δd of the surface disordered and liquid layers of Cu and Ta and (b) the liquid-solid interface velocity of Cu and Ta versus temperature during melting process. Since the length of the sample changes during heating, we normalize Δd by the length of sample at each temperature. Below premelting, Δd measures the disordered crystalline surface mean position.

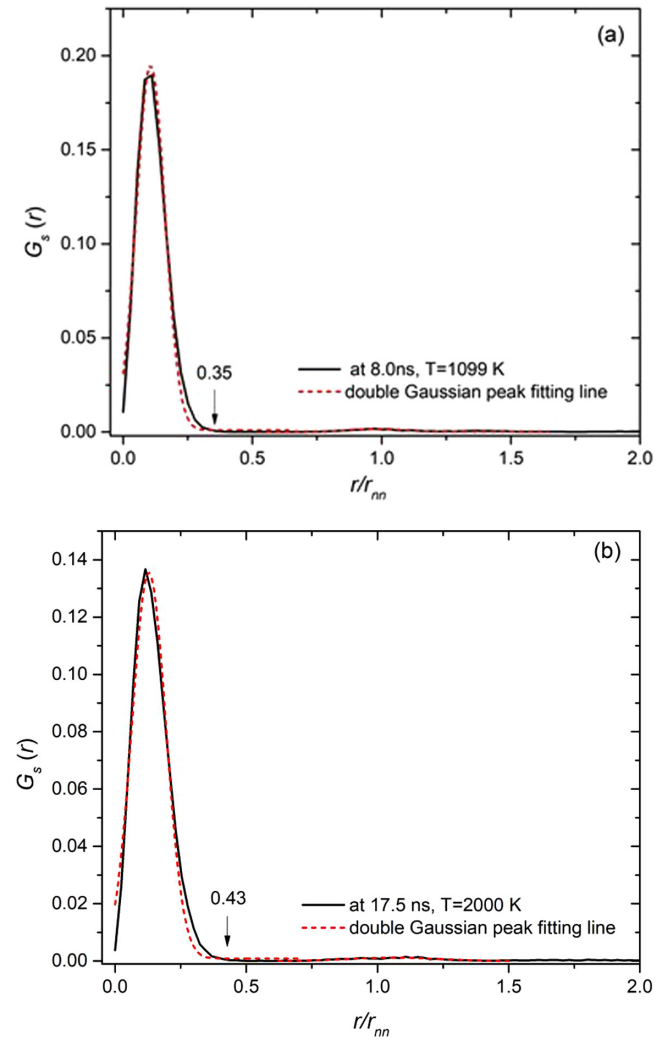

FIG. 5. The probability for particle displacement described by van Hove function $G_s(r, t)$ at 1099 K of Cu (a) and 2000 K of Ta (b) that are used to define mobile atoms.

resistance to delocalization throughout the temperature range until premelting, whereas that of Ta grows steadily with a nearly constant velocity [Fig. 4(b)].

In the following, we show that the different kinetic behavior of the surface disordered and liquid layers for bcc Ta and fcc Cu is related to the underlying crystal structure: the more densely packed fcc crystal surface prefers to have a layer of disordered or liquid staying in a constant thickness, or being localized once it forms, while the more open or loosely packed bcc crystal exhibits growth, or delocalization. The underlying reason is related to their unique atomic mechanism of surface mediated melting, i.e., formation and kinetics of the correlated atomic configurations.

D. Correlated atomic motion as a mechanism for surface mediated melting

Melting is an atomic position disordering process with atoms being displaced out of their lattice positions by thermal agitation. Therefore, this process is thought to be random and chaotic. Recent works have revealed a more detailed atomic process in bulk as well as surface mediated melting where highly correlated atomic motions are involved [29]. Instead of carrying out independent or random displacement, atoms in the heated crystals form extended, or correlated atomic configurations in the form of atomic chains or loops; and these atoms move collectively. Melting is found to be related to the proliferation of those EACs. In the following, we show that the above-reported kinetic behaviors are originated from this atomic mechanism.

To identify the correlated atomic configurations, we first define the mobile atoms that have their MSDs larger than the threshold values, $0.35r_{nn}$ for fcc Cu and $0.43r_{nn}$ for bcc Ta as shown in Fig. 5, where r_{nn} is the nearest neighbor distance at a temperature. r_{nn} corresponds to the valley position between the first and the second neighbors in the corresponding crystals' RDF. When the MSD is larger than this value, the atom has moved away from its lattice position and is "mobile". If two nearest atoms are moving away from

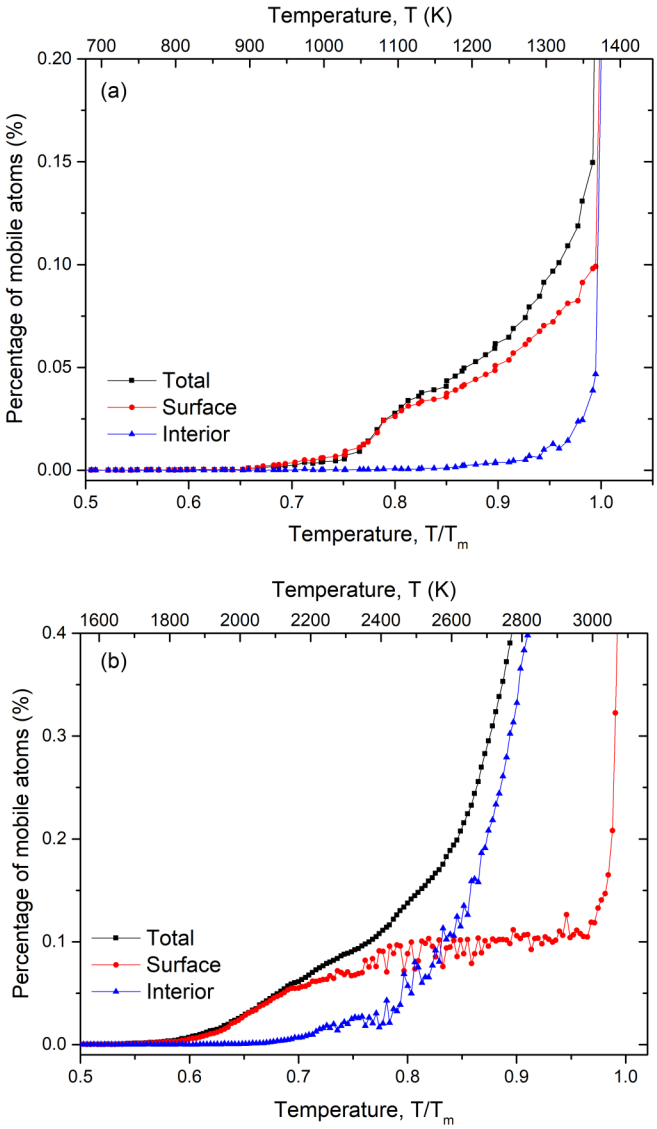

FIG. 6. The percentage of mobile atoms of the surface and bulk region for Cu (a) and Ta (b) versus temperature. The x axis of temperature is also normalized by the respective melting temperature of Cu (1364 K) and Ta (3094 K).

their respective lattice positions simultaneously, they form the unit of the correlated atomic configuration [29–32]. For example, mobile atom i and j form a collective atom displacement if they are still in each other's neighborhood, that is, $\min[|(r_i(\Delta t) - r_j(0)|, |(r_i(0) - r_j(\Delta t)|] < r^*$, the threshold r^* is $0.35r_{nn}$ for fcc Cu and $0.43r_{nn}$ for bcc Ta shown in Fig. 5. By identifying all possible units that are moving together, we can map out the correlated atomic motions involved in melting. As shown below, these units take two forms, chain or loop.

Figures 6(a) and 6(b) show the number fraction of mobile atoms in the surface region and the interior of the sample excluding the surfaces for Cu and Ta. At low temperature, there are few mobile atoms present as both the surface and the interior remain in a crystalline state. As the temperature increases, above about $0.65T_m^{\text{surf}}$ for Cu and $0.54T_m^{\text{surf}}$ for Ta, the number of mobile atoms in the surface region begins to increase; and the onset of its rise coincides precisely with the surface disordering temperatures observed in α_2 and MSD in Fig. 1. In general, one finds that at each given temperature below the bulk melting point, there are more mobile atoms on the surfaces than in the bulk. At the premelting temperature, the surface mobile atoms proliferates and at the bulk melting point, their number increases dramatically.

Another intriguing observation is the difference in the temperature dependence of the number of mobile atoms in the surface region, as well as the interior, between fcc Cu and bcc Ta: At the onset of surface disordering, the fraction of the mobile atoms on Cu (100) surface quickly rises up and continues to increase with the increasing temperature. Since the slope of the curve gives the rate of the production of the mobile atoms, one can see in Fig. 6(a) that the fcc Cu surface, once becomes disordered, will continue with the disordering with a steady growth rate of the mobile atoms. In contrast, the interior region shows little change, i.e., the number of the mobile atoms remains nearly negligible until the bulk melting is approached. The sample finally melts when the number of the surface mobile atoms diverge at the bulk melting point.

Ta shows just the opposite behavior: Once formed at a slightly lower onset temperature at $0.65T_m^{\text{surf}}$ the surface disordering reaches a plateau with nearly a constant number fraction of the surface mobile atoms [Fig. 6(b)]. In the meantime, the number of mobile atoms in the interior of the sample starts to increases rapidly at about $0.67T_m^{\text{surf}}$ with the increasing temperature. The number of the mobile atoms inside the sample quickly dominates the overall disordering process including the final melting: At about $0.85T_m^{\text{surf}}$, the number of the mobile atoms inside the sample outgrows rapidly and passes that of the surface which remains nearly unchanged. In the following, we give the reasons behind these observations, and other results presented early. One is the strong dependence of surface disordering and melting on the underlying crystal structure, and the second is the atomic mechanism of melting resulted from the formation and kinetics of the collective atomic configurations.

Since the (100) plane of the fcc Cu is denser than that of the bcc Ta, the latter becomes disordered relatively easily under thermal agitation. Hence Ta has the lower surface disordering temperature and the relatively higher number fraction of mobile atoms compared to that of Cu [Fig. 6(a)] and the quick saturation of surface disordering by the number of surface mobile atoms [Fig. 6(b)]. The same reason is also behind the change of the interior mobile atoms. As shown in Fig. 6(b), mobile atoms start to form inside the Ta crystal as soon as the surface disordering just becomes saturated, or reaches the plateau region at about $0.85T_m^{\text{surf}}$. The fraction of the mobile atoms formed inside the crystal increases exponentially with the increasing temperature, while that of the surface remains a constant. Apparently, the easy generation of disordering allows the surface as well as the interior to disorder easily because of its more open structure. As a comparison, the more close packed the fcc crystal, the harder it is for Cu to generate disordering, as compared to Ta on surface, and even more difficult inside the crystal, which requires a longer time, or higher temperature to accomplish. Therefore, the underlying crystal structure plays an important role in the different

kinetic behaviors of surface and bulk disordering during surface mediated melting.

The difference in melting kinetics during heating is also manifested through the unique atomic mechanisms through the correlated atomic movement for the EACs formed by the mobile atoms. When an atom vibrates with an amplitude larger than a threshold value, it presumably moves out of the equilibrium lattice position. The atomic motion does not appear to be completely random as thought [30]. Instead, each atomic motion is correlated to another atom's movement, collectively they form the extended atomic configurations of the mobile atoms that are moving synchronously. Our early work [17,21] established the connection between these collective motion of the extended atomic configurations and melting transition in perfect crystals without surfaces: When a sufficient amount of these EACs are formed, their mutual interaction becomes intense enough to break the crystal structure and hence causes melting. The same mechanism appears to act similarly here in surface mediated melting. Figures 7(a)–7(d) show the snapshots of the correlated atomic motion. One can see the atomic chains and loops in Cu and Ta at different temperatures. For better visualization, we plot both the top and side perspective views of the samples, so one can see the EACs on the surface and inside the samples clearly.

As shown in Fig. 7(a), for Cu the EACs form primarily on the surface and as the temperature increases, more EACs appear on the surface [Fig. 7(b)] and little forms in the interior of the crystal [Fig. 7(e)], even at relatively high temperature close to the bulk melting point at $0.95T_m^{\text{surf}}$ [Fig. 7(f)]. For Ta, the situation is just opposite: The EACs form on the surface at relatively lower temperature and quickly become saturated to a plateau value [Figs. 7(c) and 7(d)]. At higher temperatures, more EACs start to appear on the surface and also inside the sample [Figs. 7(g) and 7(h)].

Note that in both Cu and Ta, most of the EACs inside the crystals are originated from the free surfaces; and the surfaces are the source mediating EACs that subsequently permeate to the inside of the samples. The EACs in Ta form both chains and loops [Figs. 7(g) and 7(h)], while those of Cu mostly chains and a few loops which can be seen clearly in Figs. 7(e) and 7(f). The difference in this behavior is quantified by the number of the chains and loops at each given temperature as shown in Fig. 8. The EACs start to form at the corresponding surface disordering temperature with the chains emerging first and followed by the loops. In general, there are more chains than loops. For Cu, a few loops form, and even when they form, the loops are mostly confined to the surface, forming the rings beginning and ending on the surfaces [see Figs. 7(e) and 7(f)]; while for Ta, both chains and loops form that emit from the surface to the bulk [see Figs. 7(g) and 7(h)].

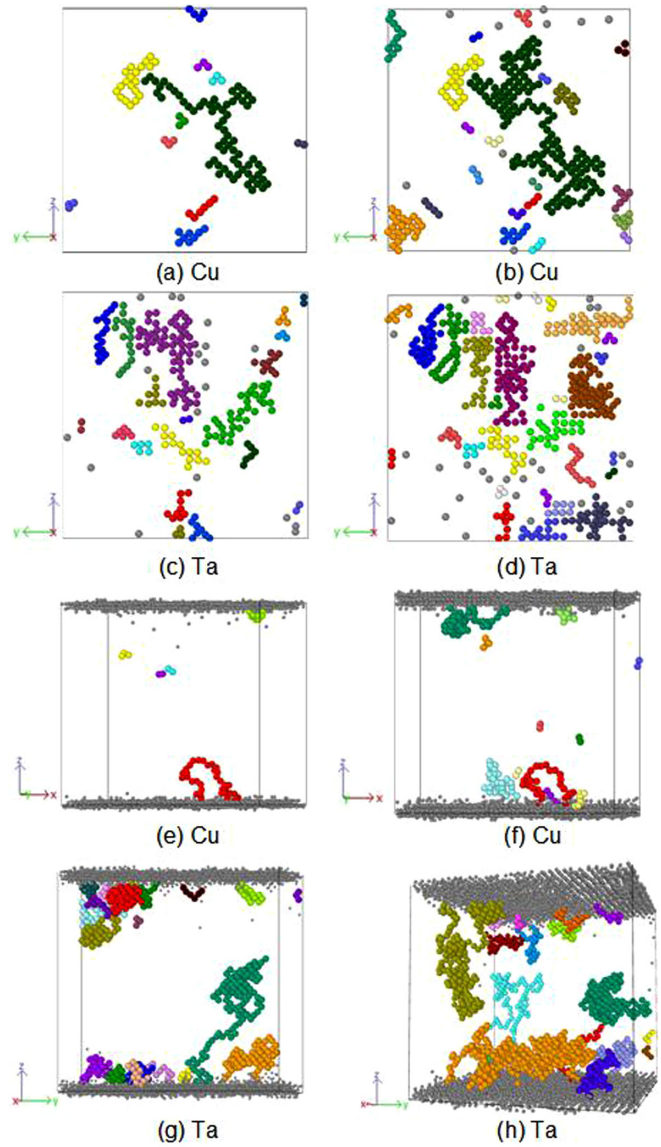

FIG. 7. The snapshots of the extended atomic configurations of the loops and chains that execute the correlated diffusive atomic motion on crystal lattices for the fcc Cu and bcc Ta with the (100) surface at different temperatures. At low temperatures, the EAC shows on the surface with top view for Cu at (a) $0.70T_m^{\text{surf}}$ and (b) $0.75T_m^{\text{surf}}$; and for Ta at (c) $0.60T_m^{\text{surf}}$ and (d) $0.62T_m^{\text{surf}}$, where T_m^{surf} is their bulk melting point in the samples with surfaces. At higher temperatures, the EACs appear inside the crystals which are plotted with the perspective view for Cu at (e) $0.90T_m^{\text{surf}}$ and (f) $0.95T_m^{\text{surf}}$; and for Ta at (g) $0.77T_m^{\text{surf}}$ and (h) $0.80T_m^{\text{surf}}$. To distinguish different chains and loops, we color them differently.

IV. DISCUSSIONS AND CONCLUSIONS

Melting starts on the surface of solids with the formation of a thin liquid layer at a lower temperature below the melting point. Further increase of temperature leads to bulk melting which is traditionally perceived as the growth of the surface liquid phase governed by the thermodynamic relation, $\gamma_{lv} + \gamma_{sl} > \gamma_{sv}$. Despite the past extensive research, the kinetics and atomic mechanisms of premelting and the surface mediated melting remain little known. In this work, using extensive atomistic modeling we provided detailed information and analysis for premelting and bulk melting mediated by surfaces. We show that at elevated temperatures, surface disorders first, followed by premelting where about a few atomic surface layers become liquid. Upon further heating, the liquid phase pervades the interior of the crystals, causing bulk melting.

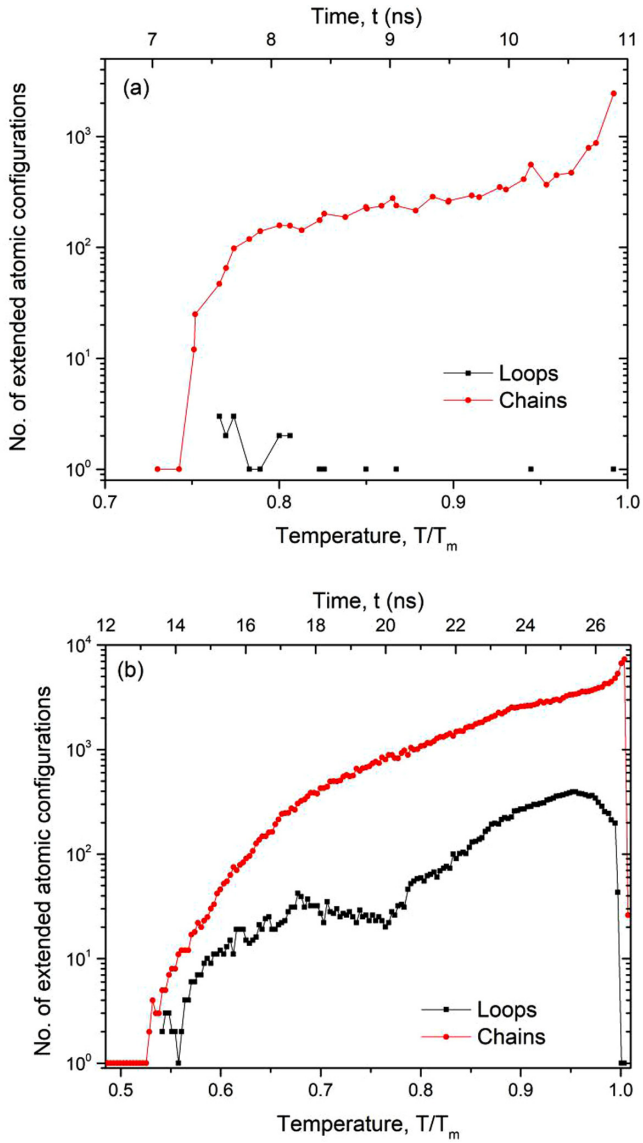

FIG. 8. The total number of the extended atomic configurations in the forms of chains and loops versus normalized temperature T/T_m^{surf} (x axis on the bottom of the figure) and time t (x axis on the top of figure in continuous heating of Cu (a) and Ta (b), where T_m^{surf} is their bulk melting point in the samples with surfaces.

Perhaps the most intriguing discovery from this work is how the surface liquid-crystal interface becomes unstable and subsequently moves into the crystal. We show that both the surface disordering and premelting depend strongly on the underlying crystal structures. The loosely packed bcc structure can promote the formation of surface disorder as well as cause disordering inside the crystal, leading to delocalization of the surface disordering during the surface mediated melting. In contrast, more densely packed fcc structure is more effective in impeding the formation and propagation of the surface disorder, resulting in a slow or sluggish movement of the surface disordered region, or localization. During this kinetics process, we found that the highly correlated atomic motion in the form of extended atomic chains and loops are carriers to spread the disorder that emit from the disordered surface and transmits to the bulk. The final melting of the entire sample is dependent on the manner of how these EACs behave, and the atomic mechanisms of surface mediated melting.

The localization and delocalization behavior for the surface premelted liquid phase will lead obviously to very different kinetic mechanisms of melting mediated by surface and melting itself as seen in the real world. For the crystals with more dense atomic packing, surface disordering is more localized and the surface melting, if it happens at all, would dominate the melting process by forming a well-defined liquid layer first. Bulk melting occurs only after the surface is completely disordered or wet, or premelts. For less dense atomic pack crystals, surface disordering occurs readily on the surface that wets the surface; at the same time, disordering inside the sample happens either through the surface mediated disorder or bulk disorder. Therefore, melting in this types of crystals can occur in a delocalized way, especially through the formation of the highly correlated EACs. These results and insights gained here will certainly help the formulation of new theories and models for crystal melting which has been baffling scientists for ages.

ACKNOWLEDGMENTS

M.L. acknowledges the support provided by the National Thousands Talents Award of China. X.F. thanks Professor Yi Liu for partial support from Materials Genome Institute of Shanghai University.

[1] E. R. Weeks, Melting colloidal crystals from the inside out, Science **338**, 55 (2012).
[2] Z. Wang, F. Wang, Y. Peng, and Y. Han, Direct observation of liquid nucleus growth in homogeneous melting of colloidal crystals, Nat. Commun. **6**, 6942 (2015).
[3] J. G. Dash, Surface melting, Contemp. Phys. **30**, 89 (1989).
[4] J. F. V. D. Veen and J. W. M. Frenken, Dynamics and melting of surfaces, Surf. Sci. **178**, 382 (1986).
[5] J. G. Dash, Melting from one to two to three dimensions, Contemp. Phys. **43**, 427 (2002).
[6] W. Theis and K. Horn, Surface premelting in Al(110) observed by core-level photoemission, Phys. Rev. B **51**, 7157 (1995).
[7] H. Dosch, T. Höpfer, J. Peisl, and R. L. Johnson, Synchrotron x-ray scattering from the Al(110) Surface at the onset of surface melting, Europhys. Lett. **15**, 527 (1991).
[8] D. M. Zhu and J. G. Dash, Surface Melting and Roughening of Adsorbed Argon Films, Phys. Rev. Lett. **57**, 2959 (1986).
[9] J. W. Gibbs, On the equilibrium of heterogeneous substances, in *Transactions of the Connecticut Academy of Arts and Sciences* (Morehouse & Taylor, New Haven, CT, 1876), p. 108.
[10] G. Bilalbegovic, F. Ercolrssi, and E. Tosatti, Orientational phase separation for vicinal surfaces close to the nonmelting Pb(111) face, Europhys. Lett. **17**, 333 (1992).

[11] H. Hakkinen and M. Manninen, Computer simulation of disordering and premelting of low-index faces of copper, Phys. Rev. B **46**, 1725 (1992).
[12] H. Hakkinen and U. Landman, Superheating, Melting, and Annealing of Copper Surfaces, Phys. Rev. Lett. **71**, 1023 (1993).
[13] R. Kojima and M. Susa, Surface melting of copper with (100), (110), and (111) orientations in terms of molecular dynamics simulation, High Temp. High Pressure **34**, 639 (2002).
[14] S. Plimpton, Fast parallel algorithms for short-range molecular dynamics, J. Comput. Phys. **117**, 1 (1995).
[15] Y. Mishin, M. J. Mehl, D. A. Papaconstantopoulos, A. F. Voter, and J. D. Kress, Structural stability and lattice defects in copper: *Ab initio*, tight-binding, and embedded-atom calculations, Phys. Rev. B **63**, 224106 (2001).
[16] R. Ravelo, T. C. Germann, O. Guerrero, Q. An, and B. L. Holian, Shock-induced plasticity in tantalum single crystals: Interatomic potentials and large-scale molecular-dynamics simulations, Phys. Rev. B **88**, 134101 (2013).
[17] X. Fan, D. Pan, and M. Li, Rethinking Lindemann criterion: A molecular dynamics simulation of surface mediated melting, Acta Mater. **193**, 280 (2020).
[18] S. Nosé, A unified formulation of the constant temperature molecular dynamics methods, J. Chem. Phys. **81**, 511 (1984).
[19] W. G. Hoover, Canonical dynamics: Equilibrium phase-space distributions, Phys. Rev. A **31**, 1695 (1985).
[20] C. Kittel, *Introduction to Solid State Physics*, 8th ed (Wiley, Hoboken, NJ, 2004).
[21] X. Fan, D. Pan, and M. Li, Melting of bcc crystal Ta without the Lindemann criterion, J. Phys.: Condens. Matter **31**, 095402 (2019).
[22] A. M. James and M. P. Lord, *Macmillan's Chemical and Physical Data* (Macmillan, Basingstoke, UK, 1992).
[23] G. E. Norman and V. V. Stegailov, Simulation of ideal crystal superheating and decay, Mol. Simul. **30**, 397 (2004).
[24] W. Kob and S. C. Glotzer, Dynamical Heterogeneities in a Supercooled Lennard-Jones Liquid, Phys. Rev. Lett. **79**, 2827 (1997).
[25] A. Rahman, Correlations in the motion of atoms in liquid argon, Phys. Rev. **136**, A405 (1964).
[26] Q. S. Mei and K. Lu, Melting and superheating of crystalline solids: From bulk to nanocrystals, Prog. Mater Sci. **52**, 1175 (2007).
[27] S. L. Zhang, X. Y. Zhang, L. Qi, L. M. Wang, S. H. Zhang, Y. Zhu, and R. P. Liu, The study of melting stage of bulk silicon using molecular dynamics simulation, Physica B **406**, 2637 (2011).
[28] S. A. Cho, Role of lattice structure on the Lindemann fusion theory of metal, J. Phys. F: Met. Phys. **12**, 1069 (1982).
[29] X. M. Bai and M. Li, Ring-diffusion mediated homogeneous melting in the superheating regime, Phys. Rev. B **77**, 134109 (2008).
[30] C. Donati and C. Glotzer, Stringlike Cooperative Motion in a Supercooled Liquid, Phys. Rev. Lett. **80**, 2338 (1998).
[31] C. Donati, S. C. Glotzer, and S. J. Plimpton, Spatial correlations of mobility and immobility in a glass-forming Lennard-Jones liquid, Phys. Rev. E **60**, 3107 (1999).
[32] H. Zhang, P. Kalvapalle, and J. F. Douglas, Stringlike collective atomic motion in the melting and freezing of nanoparticles, J. Phys. Chem. B **115**, 14068 (2011).